

# Mechanical Behaviour of an Induction Machine Stator

Lieven Vandeveldel<sup>1</sup>, Benedict Verhegghe<sup>2</sup>, Jeroen Van Cotthem<sup>1</sup>, Tom Heirman<sup>1</sup>, and Jan Melkebeek<sup>1</sup>

<sup>1</sup> Electrical Energy Laboratory (EELAB)  
Department of Electrical Energy, Systems and Automation (EESA)  
Ghent University  
Sint-Pietersnieuwstraat 41, B-9000 Ghent, Belgium  
e-mail : lieven.vandevelde@rug.ac.be

<sup>2</sup> Mechanics of Materials and Structures  
Department of Mechanical Construction and Production  
Ghent University  
Sint-Pietersnieuwstraat 41, B-9000 Ghent, Belgium  
e-mail : benedict.verhegghe@rug.ac.be

**Abstract** – This paper presents the investigation of the mechanical behaviour of an induction machine stator in relation to vibration problems. The natural frequencies and mode shapes are investigated by both finite element computations and measurements. The mechanical damping ratios of the different modes are determined experimentally.

## 1. Introduction

The (numerical) analysis of vibrations and noise of magnetic origin of electrical machines is a complex problem. In order to obtain an accurate assessment of the generated vibrations and noise, the successive steps of the computation procedure, i.e. the analyses of the magnetic field distribution, the exciting magnetic forces, the mechanical (vibrational) and acoustic behaviour, have to be carried out in detail.

In previous papers of the authors, the magnetic field and force computation in electrical machines, in particular induction motors, has been dealt with. In [1] a magnetic field and force computation technique, based on magnetic equivalent circuits, has been presented. This computation method has been applied for the force analysis in induction motors and takes into account the various effects which affect the spectral content of the magnetic forces and thus of the vibrations and noise, viz stator and rotor slotting, the winding arrangement (m.m.f. harmonics), eccentricity, saturation and harmonics of the applied voltage (e.g. inverter supply). A magnetic force computation method based on the 2D finite element technique, which may be applied to all kinds of electromagnetic devices, has been presented in [1].

The present paper focuses on the mechanical behaviour of induction motors, in particular the stator lamination stack, in relation to vibration problems. In this respect, the modal analysis is commonly applied [3, 4].

As electrical machines may have a complex mechanical structure, a step-by-step approach is adopted for the investigation of the structural behaviour of induction motors, i.e. from a stator without windings or housing to a complete standard induction motor including 3D effects (such as skewed rotor slots). In this paper, the results of the first step, i.e. the analysis of the structural behaviour of the stator lamination stack, are reported.

Both experimental and numerical investigations are pre-

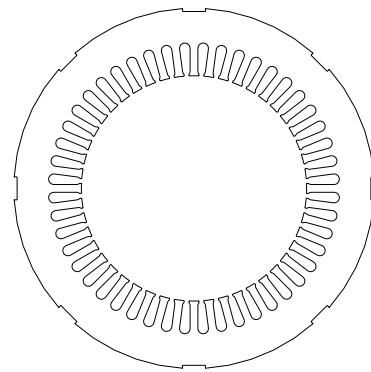


Fig. 1. Geometry of the stator

TABLE I  
GEOMETRICAL DATA OF THE STATOR

outer diameter	:	240	mm
inner diameter	:	150	mm
axial length	:	210	mm
slot depth	:	22	mm
tooth width	:	5.2	mm

sented. The computations presented in this paper have been carried out with the ABAQUS finite element software.

The device under study is the stator of an 11 kW induction motor, depicted in Fig. 1, the geometrical data of which are listed in Table 1. On the outer surface there are eight equidistant notches for the clamps which keep the lamination stack together.

## 2. Modal Analysis

If the deformation (and motion) of a structure is described by means of  $N$  degrees of freedom:

$$\mathbf{x} = [x_1 \dots x_N]^T, \quad (1)$$

the equations of motion are given by:

$$\mathbf{M}\ddot{\mathbf{x}} + \mathbf{C}\dot{\mathbf{x}} + \mathbf{K}\mathbf{x} = \mathbf{f} \quad (2)$$

where  $\mathbf{x}$  and  $\mathbf{f}$  are the displacement and force vectors ( $N \times 1$ ) respectively and  $\mathbf{M}$ ,  $\mathbf{C}$  and  $\mathbf{K}$  the mass, damping and stiffness matrices ( $N \times N$ ) respectively. By solving the eigenvalue problem determined by the undamped ( $\mathbf{C} = 0$ ) homogeneous equations (2), the matrix  $\Psi$  ( $N \times N$ ) of the normalized eigenvectors (mode shapes)  $\psi_i$  ( $N \times 1$ ) is obtained:

$$\Psi = [\psi_1 \dots \psi_N] \quad \text{with} \quad \Psi^{-1} = \Psi^T \quad (3)$$

which allows to define the generalized displacement vector  $\mathbf{q}$  and generalized force vector  $\mathbf{h}$ :

$$\mathbf{x} = \Psi \mathbf{q} \quad (4)$$

$$\mathbf{f} = \Psi \mathbf{h} \quad (5)$$

The equations of motion (2), written in terms of the generalized displacement and force vectors (4)-(5):

$$\Psi^{-1} \mathbf{M} \Psi \ddot{\mathbf{q}} + \Psi^{-1} \mathbf{C} \Psi \dot{\mathbf{q}} + \Psi^{-1} \mathbf{K} \Psi \mathbf{q} = \mathbf{h} \quad (6)$$

$$\Rightarrow \mathcal{M} \ddot{\mathbf{q}} + \mathcal{C} \dot{\mathbf{q}} + \mathcal{K} \mathbf{q} = \mathbf{h} \quad (7)$$

where  $\mathcal{M}$  and  $\mathcal{K}$  are diagonal matrices, may be uncoupled if proportional damping is assumed such that also  $\mathcal{C}$  is diagonal. In this case, for each mode  $i$ , the following equation is found according to (7):

$$m_i \ddot{q}_i + c_i \dot{q}_i + k_i q_i = h_i \quad (i = 1, \dots, N) \quad (8)$$

or in the Laplace domain:

$$m_i (s^2 + 2\xi_i \omega_i s + \omega_i^2) Q_i(s) = H_i(s) \quad (9)$$

where  $m_i$ ,  $\xi_i$  and  $\omega_i = \sqrt{k_i/m_i}$  are the modal mass, damping ratio and natural pulsation respectively.

According to (4), (5) and (9), the solution of the equations of motion (2) in the Laplace domain is given by:

$$\mathbf{X}(s) = \mathcal{G}(s) \mathbf{F}(s) \quad (10)$$

where the transfer matrix  $\mathcal{G}(s)$  is given by:

$$\mathcal{G}(s) = \sum_{i=1}^N \frac{\psi_i \psi_i^T}{m_i (s^2 + 2\xi_i \omega_i s + \omega_i^2)} \quad (11)$$

### 3. Finite Element Structural Analysis

#### A. Two-Dimensional FE models

The natural frequencies and mode shapes were computed by using a 2D plane stress finite element model, where the mass density of the steel is  $\rho=7800 \text{ kg/m}^3$  and where the elasticity constants are given by the Young modulus  $E = 210 \text{ GPa}$  and the Poisson ratio  $\nu = 0.28$ . Damping was not considered.

At first instance, the eight notches in the stator mentioned before were neglected in the FE model. Different FE meshes consisting of first order triangular elements and with increasing number of nodes were used for computing the first 40 natural frequencies and mode shapes  $\psi_i$ .

The first 10 natural frequencies, computed by using the different meshes and by assuming a plane stress condition, are listed in Table II. We remark that the computed natural

TABLE II  
COMPUTED NATURAL FREQUENCIES (HZ) – 2D MODEL  
WITHOUT NOTCHES

mode	order	number of nodes			
		8413	12350	26774	40078
1,2,3	-	0	0	0	0
4a	2	1072.3	1063.2	1056.4	1054.5
4b	2	1072.4	1063.3	1056.4	1054.5
5a	3	2834.5	2910.5	2792.3	2787.4
5b	3	2835.2	2810.7	2792.4	2787.4
6a	4	4943.4	4897.1	4858.4	4848.3
6b	4	4943.8	4897.3	4858.5	4848.4
7	0	6546.4	6530.4	6521.8	6519.0

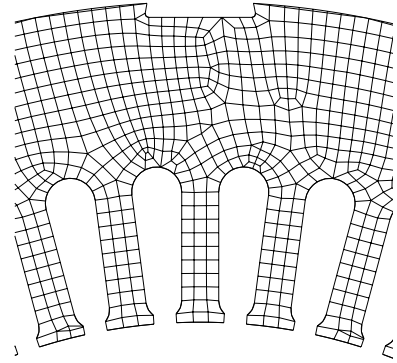


Fig. 2. 2D FE mesh

frequencies decrease with increasing accuracy of the mesh (increasing number of nodes). Indeed, the mechanical stiffness of the structure is overestimated by the FE discretization which results in an overestimation of the natural frequencies.

Modes 1, 2 and 3 correspond to movements as a rigid body (2 translations and 1 rotation), as no boundary conditions inhibiting these displacements were imposed. The mode shapes of the modes with the lowest natural frequencies can be characterized as radial deformations of order 2, 3, 4 and 0. Due to the geometrical symmetry, nonzero order modes form pairs, indicated with  $a$  and  $b$ , with the same natural frequency and with mode shapes which are rotated over a quarter of a period.

Next, a 2D FE model including the notches has been built. A detail of the mesh, using second order quadrilaterals (and a few triangles) is shown in Fig.2. The results obtained by assuming plane stress or plane strain are listed in Table III.

As expected, the natural frequencies obtained for the model with notches are (under the same conditions of plane stress) lower than those for the model without notches. It should be noted however that the frequencies for modes 6a and 6b (order 4) now have different values. This can easily be explained by observing the mode shapes in Fig. 3. Other low order modes still occur in pairs.

The mode shapes corresponding with the other computed natural frequencies are higher order radial deforma-

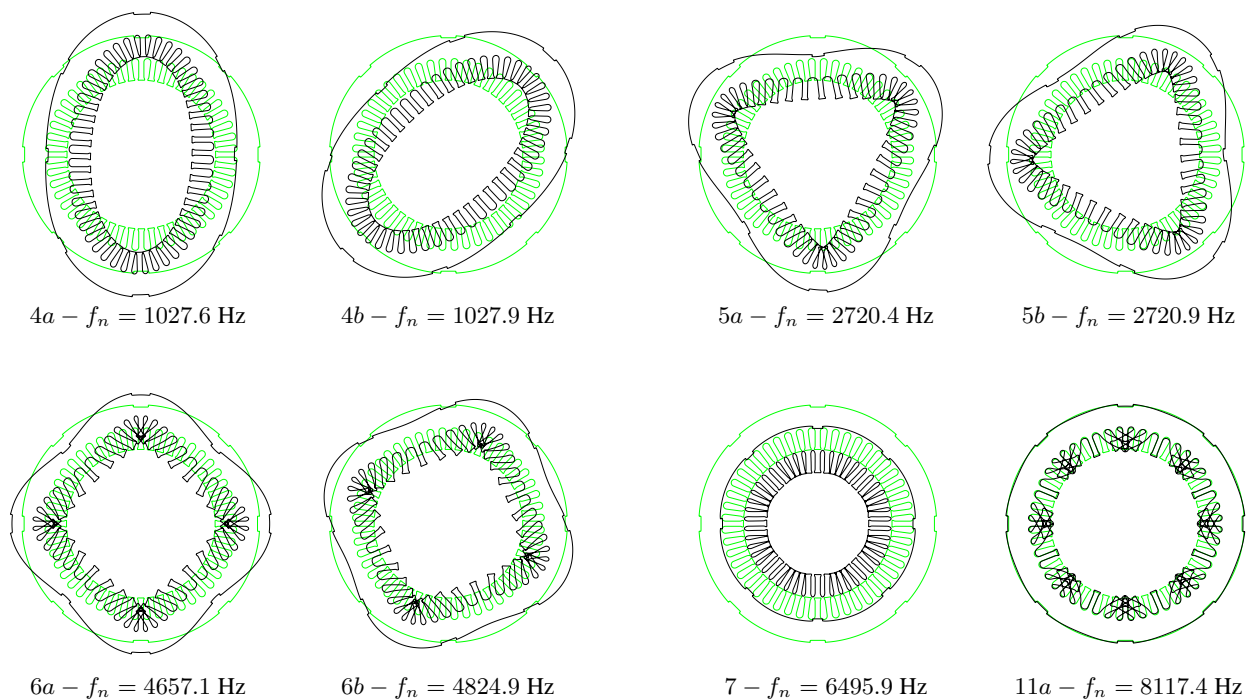


Fig. 3. Computed mode shapes and natural frequencies for the 2D model with notches

TABLE III  
COMPUTED NATURAL FREQUENCIES (HZ) – 2D MODEL WITH NOTCHES

mode	order	plane stress	plane strain
1,2,3	-	0	0
4a	2	1027.6	1070.0
4b	2	1027.9	1070.0
5a	3	2720.4	2830.4
5b	3	2720.9	2830.4
6a	4	4657.1	4843.7
6b	4	4824.9	5016.8
7	0	6495.9	6750.8

tions or are determined by the deformation of the teeth rather than the yoke, e.g. mode 11a depicted in Fig. 3.

### B. Three-Dimensional FE model

In order to investigate possible 3D effects on the natural frequencies, a 3D model of the stator was built as well. For the sake of simplicity, the stator was modelled by means of isotropic material, i.e. by neglecting its laminated structure. The 3D mesh consists of hexahedral elements and has 30 layers in the axial direction. The number of nodes is 96689.

In Table IV the modes indicated with \* refer to mode shapes where the radial displacements of both ends of the stack are shifted over half a period. This is illustrated in Fig. 4 for mode 8a, 11a and 13a. The other modes correspond to those obtained with the 2D model. The natural frequencies obtained with the 3D model are similar to those obtained with the 2D model for plane strain.

TABLE IV  
COMPUTED NATURAL FREQUENCIES – 3D MODEL

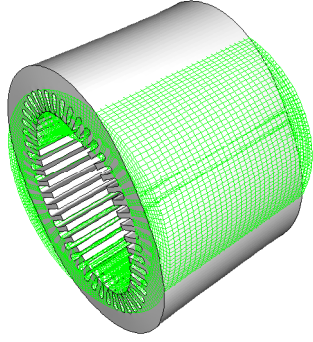
mode	order	natural frequency (Hz)
1,2,3,4,5,6	-	0
7a	2	1082.4
7b	2	1083.0
8a	2*	1463.2
8b	2*	1463.4
9a	3	2853.6
9b	3	2854.9
10a	3*	3379.0
10b	3*	3379.5
11a	1*	4881.7
11b	1*	4882.5
12a	4	4899.4
12b	4	4903.9
13a	4*	5370.4
13b	4*	5377.3

## 4. Experimental Determination of Natural Frequencies, Mode Shapes and Damping

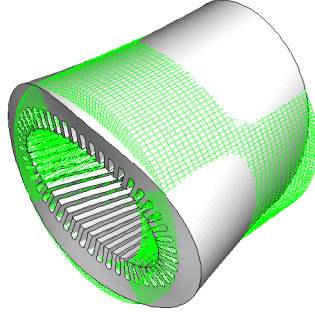
### A. Excitation Sources

For the experimental investigation of the mechanical different kinds of excitation may be used.

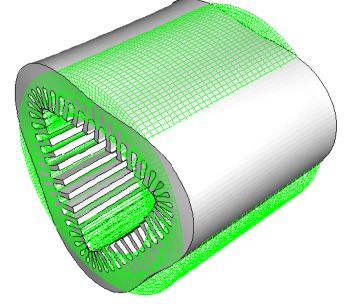
In case of electrical machines, an obvious choice is to feed one of the windings with a current  $I$ . The magnetic forces are proportional to the square of the induction  $B$ , and thus to the square of the current  $I$  if saturation can be ne-



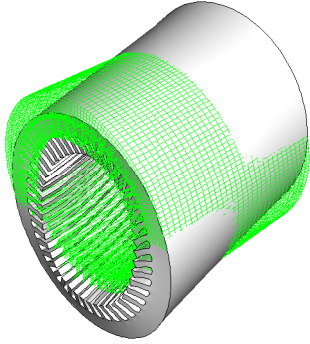
7a -  $f_n = 1082.4\text{Hz}$



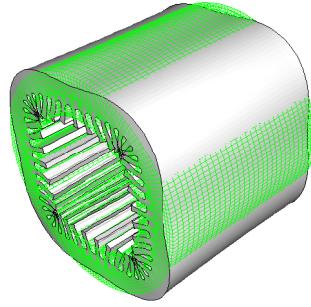
8a -  $f_n = 1463.2\text{Hz}$



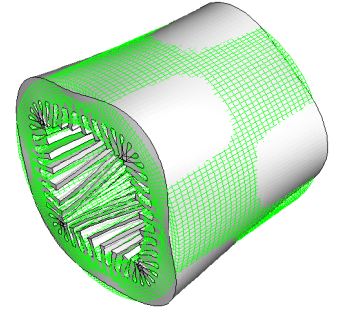
9a -  $f_n = 2853.6\text{Hz}$



11a -  $f_n = 3379.0\text{Hz}$



12a -  $f_n = 4899.4\text{Hz}$



13a -  $f_n = 5370.4\text{Hz}$

Fig. 4. Some computed mode shapes (3D model)

glected (at low  $B$ ). If the current  $I$  has the following form:

$$I = a + b \sin(\omega t) \quad (12)$$

the magnetic force is determined by

$$\begin{aligned} F &\propto B^2 \\ &\propto I^2 \\ &\propto \left( a^2 + \frac{b^2}{2} \right) + 2ab \sin(\omega t) + \frac{b^2}{2} \cos(2\omega t) \end{aligned} \quad (13)$$

By choosing  $b \ll a$  such that the third term of 13 (double frequency) is negligible in comparison to the second term (single frequency) and by varying the frequency  $\omega$  (e.g. by applying a *swept sine*), the frequency response between the vibration and the current can be measured, which is a good assessment of the frequency response between the vibration and the magnetic force. One of the advantages of an electromagnetic excitation is the fact that the applied force is similar to the force during the normal operation of the machine.

Also an electromagnetic exciter with a force transducer, which excites the structure in a single point, may be used. For the experiments described in this paper, a hand-held exciter has been used such that the stator can easily be excited in different points. This allows to determine the mode shapes by vibration measurements in only one or a few points of the surface.

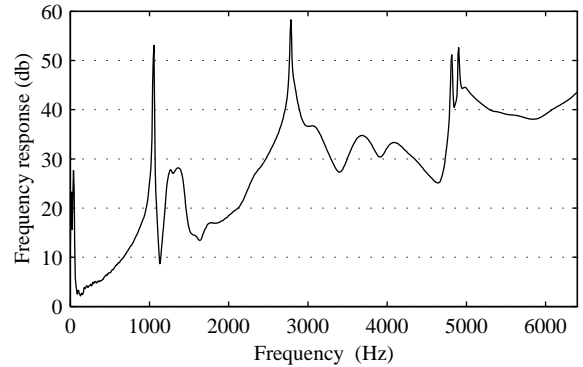


Fig. 5. Frequency response function (acceleration vs. applied force)

### B. Frequency Response Function

Figure 5 shows the measured frequency response function (FRF) of the vibration in a point of the stator surface vs. the force applied in another point by means of the electromagnetic exciter, in the frequency range 0 - 6.4 kHz.

The most important peaks in Fig.5 occur at frequencies of approximately 1050 Hz, 2785 Hz, 4820 Hz, and 4900 Hz. These frequencies correspond with the modes of order 2, 3 and 4 found by the numerical analyses, the results of which were summarized in Tables III and IV. These vibration modes will further be investigated in more detail. We

already remark that the difference between the natural frequencies of the fourth order modes (6a and 6b) obtained by means of a 2D model with notches is clearly observed in the measured FRF of Fig.5 (two distinct peaks at approx. 4820 Hz and 4900 Hz).

### C. Natural Frequencies and Damping

When considering  $n$  modes with neighbouring natural pulsations  $\omega_i$  ( $i = 1, \dots, n$ ), the transfer function for the acceleration in point  $k$  vs. the force applied in point  $l$  is approximately given by

$$g_{kl}(j\omega) = \sum_{i=1}^n a_i \frac{-\omega^2}{-\omega^2 + 2\xi_i \omega_i j\omega + \omega_i^2} + (b_1 + b_2 j) + (c_1 + c_2 j) \omega^2 \quad (14)$$

for pulsations  $\omega$  near the considered natural frequencies  $\omega_i$ . Herein the last terms of the right hand side account for the contribution of the modes  $k$  for which  $\omega_k \gg \omega$  and  $\omega_k \ll \omega$ .

The natural pulsation  $\omega_i$  and damping ratio  $\xi_i$  of some modes have been determined by fitting the parameters of (14) to measured FRFs in a least-squares sense by using the Matlab 'lsqcurvefit' function.

In Fig. 6 (a) the magnitudes of a measured frequency response and of the fitted function in the range 1000-1100 Hz are shown. Apparently there are two neighbouring natural frequencies in this frequency range. Therefore a curve-fitting problem according to (14) with  $n = 2$  was solved. The measured and fitted curves are almost identical. Even if the two natural frequencies cannot be clearly distinguished, e.g. in the FRF of Fig. 6 (b), curve fitting is still possible.

Figure 6 (c) shows a measured and fitted FRF in the range 4750-4950 Hz. Here three modes have to be taken into account ( $n=3$ ).

The natural frequencies and damping ratios, obtained by applying curve fitting on the basis of (14), are listed in Table V

In comparison with the results computed with the 2D model with notches (Fig. 3 and Table III), additional modes are observed experimentally. For instance, for the second and third order modes, only a single natural frequency was found by the FE analysis, viz 1070 Hz and 2830.4 Hz for order 2 and 3 respectively (by assuming plane strain). The experiments reveal for both modes a pair of natural frequencies (Table V). For the fourth order mode two neighbouring natural frequencies were obtained numerically (4843 Hz and 5016 Hz), while three different modes were observed (Fig. 6 (c) and Table V).

### D. Mode Shapes

For the experimental determination of the mode shapes, we consider the radial displacements of  $N$  discrete points on a circular contour in the middle of the stator. When the excitation frequency is near the natural frequency of mode  $i$ , the transfer matrix  $\mathcal{G}(j\omega)$  is dominated by this eigenmode. The acceleration is measured in a single point  $k$  while the structure is consecutively excited in the  $N$  points. This way,

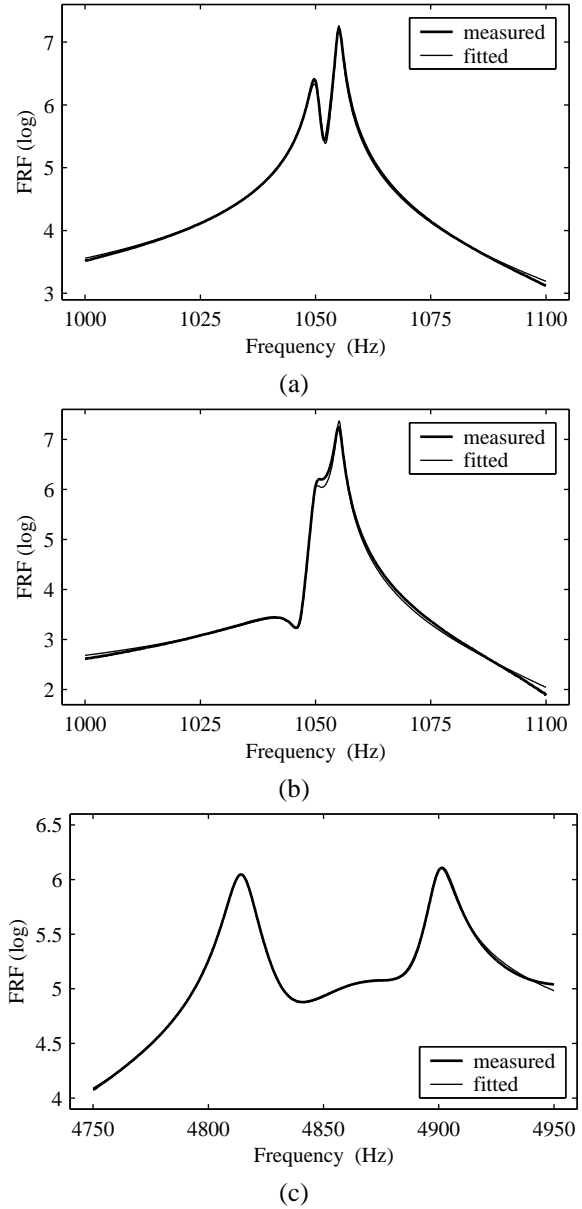


Fig. 6. Measured and fitted frequency response functions

TABLE V  
NATURAL FREQUENCIES AND DAMPING RATIOS OBTAINED BY  
CURVE FITTING

order	$f_i$ (Hz)	$\xi_i$
2	1050	0.00139
2	1055	0.000548
3	2782	0.0015
3	2790	0.0014
4	4815	0.0013
4	4868	0.0078
4	4900	0.00116

the  $k$ -th row of the transfer matrix  $-\omega^2 \mathcal{G}(j\omega)$  is measured, which is for  $\omega \approx \omega_i$  approximately given by :

$$\frac{-\omega^2 \psi_i^k}{m_i (-\omega^2 + 2\xi_i \omega_i j\omega + \omega_i^2)} \psi_i^T \quad (15)$$

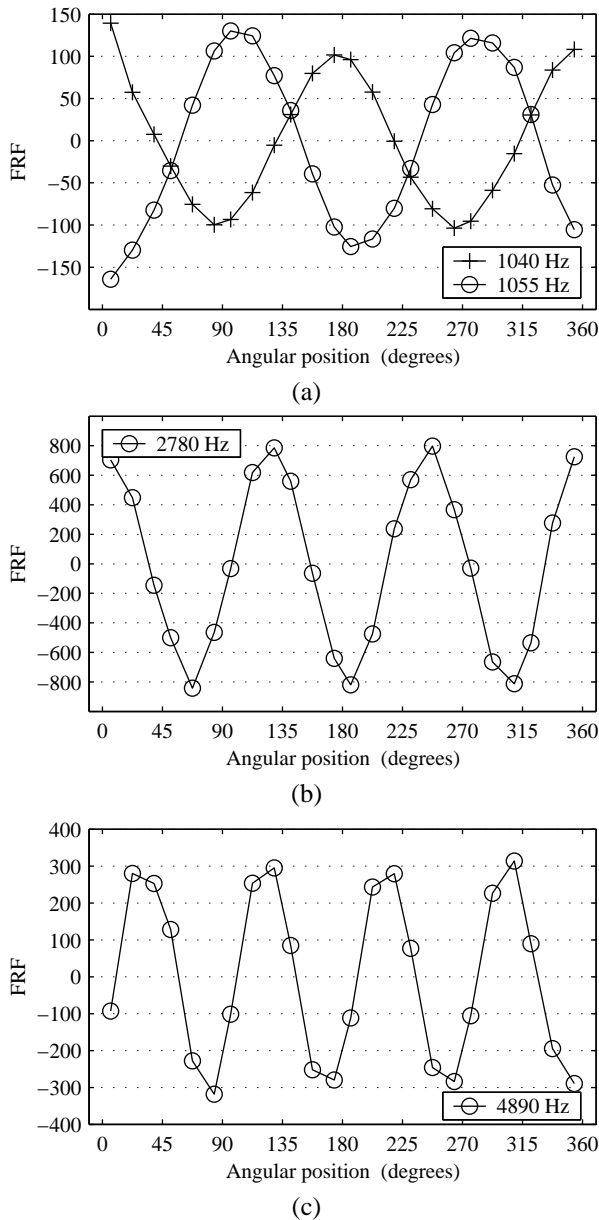


Fig. 7. Measured mode shapes (real part of the frequency response vs. the angular position of the excitation points)

which is thus a measure of the  $i$ -th mode shape:

$$\psi_i = [\psi_i^1 \dots \psi_i^N]^T. \quad (16)$$

The mode shapes corresponding with the peaks in the FRF at approximately 1050 Hz, 2785 Hz, and 4850 Hz were measured by exciting the stator in  $N = 24$  points. Figure 7 (a) shows the real part of the frequency responses vs. the angular position of the 24 points for two frequencies near

1050 Hz. The excited vibration clearly has a second order mode shape for these frequencies, which corresponds with the computed modes 4 and 7 obtained by the 2D and 3D computations respectively. Remark the phase shift of approximately  $180^\circ$  between the curves for 1040 Hz and 1055 Hz.

Figures 7 (b) and (c) show the real part of the frequency responses in the 24 points for 2780 Hz and 4890 Hz respectively. The observed vibrations reveal the computed third order mode shapes of modes 5 (2D model) and 7 (3D model) and the fourth order mode shapes of modes 6 (2D model) and 12 (3D model).

## 5. Conclusion

A detailed investigation of the mechanical behaviour of an induction machine stator has been carried out by both finite element computations and experiments. This research will be continued by modelling the stator with windings and finally a complete induction machine.

## Acknowledgement

This research has been carried out with the financial support of the Fund for Scientific Research - Flanders (Belgium) (F.W.O.-Vlaanderen) and in the frame of the Interuniversity Attraction Poles (IAP P4/20 – P5/34) supported by the Belgian government.

L. Vandeveld is a Postdoctoral Fellow of the Fund for Scientific Research - Flanders.

## References

- [1] L. Vandeveld, J. Gyselinck, and J. Melkebeek, "Electromechanical Analysis of Vibrations and Noise of Squirrel-Cage Induction Motors," in *Proceedings International Conference on Electrical Machines (ICEM '98)*, Istanbul, Turkey, 2-4 September 1998, Vol. 1, pp. 496-501
- [2] L. Vandeveld, J. Gyselinck, and J. Melkebeek, "Long-range magnetic force and deformation calculation using the 2D finite element method," *IEEE Transactions on Magnetics*, Vol. 34, No. 5, September 1998, pp. 3540-3543
- [3] S. P. Verma and A. Balan, "Experimental investigations on the stators of electrical machines in relation to vibration and noise problems," *IEE Proceedings - Electrical Power Applications*, Vol. 145, No. 5, September 1998, pp. 455-461
- [4] C. G. C. Neves, R. Carlson, N. Sadowski, J. P. A. Bastos, N. S. Soeiro, and N. S. Y. Gerges, "Experimental and Numerical Analysis of Induction Motor Vibrations," *IEEE Transactions on Magnetics*, Vol. 35, No. 3, May 1999, pp. 1314-1317